DALTON

Conformational change of the *N,N'*-bis(3-aminopropyl)oxamidate ligand in nuclearity tailoring copper(II) complexes †

José Luis Sanz,[a] Beatriz Cervera,[a] Rafael Ruiz,[a] Claudette Bois,[b] Juan Faus,[a] Francesc Lloret*[,a] and Miguel Julve[a]

[a] *Departament de Química Inorgànica, Facultat de Química de la Universitat de València, Dr. Moliner 50, 46100 Burjassot (València), Spain*
[b] *Laboratoire de Chimie des Métaux de Transition, URA 419 CNRS, Université Pierre et Marie Curie, 75252 Paris, France*

N,N'-Bis(3-aminopropyl)oxamide (H_2L^1) which can adopt *cis* and *trans* conformations reacted with copper(II) salts in its deprotonated form to yield the compounds $[CuL^1]$ **1**, $[Cu_3L^1{}_2(NO_3)_2]\cdot H_2O$ **2**, $[Cu_2L^1(NO_3)_2]$ **3** and $[Cu_2L^1(O_2CMe)_2]\cdot 2H_2O$ **4**. The structures of **1**, **3** and **4** have been determined by single-crystal X-ray diffraction methods. That of **1** consists of mononuclear $[CuL^1]$ units where the oxamidate is in a *cis* conformation co-ordinated to the copper atom through its four nitrogen atoms. The copper surroundings are close to square planar. The amidate–copper bond distance [1.955(6) Å] is significantly shorter than that involving the amine group [1.999(7) Å]. The structures of **3** and **4** comprise centrosymmetric *trans* oxamidate-bridged copper(II) dinuclear units which are linked by asymmetric bis(monodentate) nitrate (**3**) and acetate (**4**) ligands to yield a sheet-like polymer (**3**) and an alternating chain (**4**). The co-ordination geometry around each copper atom is distorted square pyramidal: the equatorial plane comprises the oxygen and nitrogen atoms of the amide, the nitrogen atom of the amine group and an oxygen atom from nitrate (**3**) or acetate (**4**) ligands. The apical position is filled by an oxygen atom from another nitrate (**3**) or acetate (**4**) group. The copper–copper separations across the oxamidate are 5.190(1) and 5.244(1) Å for **3** and **4**, respectively, and those across the nitrato and acetato groups are 5.116(1) and 3.350(1) Å. Variable-temperature magnetic susceptibility measurements show a Curie law behaviour for **1** and the occurrence of a strong antiferromagnetic coupling through the oxamidate bridge in **2**–**4** ($J = -325$, -393 and -305 cm^{-1}, respectively). The versatility of L^1 as a ligand and its ability to mediate strong antiferromagnetic interactions is analysed and discussed.

N,N'-Bis(3-aminopropyl)oxamide (H_2apoxd, H_2L^1) is a well known member of the *N,N'*-disubstituted oxamides the co-ordination chemistry of which has been explored in the last decade.[2–13] The great versatility of apoxd^{2-} as a ligand is due to the adoption of either *cis* or *trans* conformations in its metal complexes, exhibiting tetradentate and bis(terdentate) co-ordination modes, respectively. In the case of copper(II) ion, potentiometric studies in aqueous solutions allowed the thermodynamic characterization of these co-ordination modes: the high values of the stability constants for the mononuclear $[CuL^1]$ [$\log \beta = 20.33(2)$] and dinuclear $[Cu_2L^1]^{2+}$ [$\log \beta = 28.15(2)$] complexes[8] illustrate the great selectivity of this kind of ligand for copper(II). The high stability in solution of $[CuL^1]$ and the fact that it can act as a bidentate ligand through its two carbonyl-oxygen atoms when the *cis* conformation is retained make it a very suitable building block to prepare homo- and hetero-di- $[CuL^1M]^{m+}$,[2,3,5,7–11] tri- $[(CuL^1)_2M]^{m+}$,[3] tetra- $[(CuL^1)_3M]^{m+6}$ and penta-nuclear $[(CuL^1)_4M]^{m+12}$ complexes. It should be noted that, in the case of the apoxd-bridged copper(II) dinuclear complexes, the only way to keep the *cis* conformation of apoxd is to block the second copper(II) ion with adequate peripheral chelating ligands. This strategy was used to prepare the structurally characterized complexes $[CuL^1Cu(bipy)][ClO_4]_2$,[2] $[CuL^1Cu(pedien)][ClO_4]_2$[2] and $[CuL^1Cu(phen)][ClO_4]_2$,[7b] where bipy = 2,2'-bipyridine, pedien = *N,N,N',N'',N''*-pentaethyldiethylenetriamine and phen = 1,10-phenanthroline. As far as the dinuclear $[Cu_2L^1]^{2+}$ unit is concerned,[13] it could easily be polymerized through the replacement of the equatorially and the two axially bound water molecules by suitable bridging ligands. This strategy has proved useful in the preparation of neutral chains of copper(II) ions with alternating bridges of oxamidato and either acetato, $[Cu_2L^2(O_2CMe)_2]$,[14] cyanato, $[Cu_2L^1(NCO)_2]$[8], or azide groups, $[Cu_2L^3(N_3)_2]$ and $[Cu_2L^4(N_3)_2]$[15,16] {H_2L^2 = *N,N'*-bis(3-amino-2,2-dimethylpropyl)-oxamide, H_2L^3 = *N,N'*-bis[(3-(methylamino)propyl]oxamide and H_2L^4 = *N,N'*-bis[2-(dimethylamino)ethyl]oxamide}.

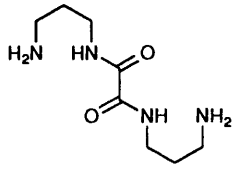

H_2L^1

In the present work, we have structurally characterized the *cis* and *trans* conformations of the apoxd^{2-} ligand in four copper(II) complexes of formula $[CuL^1]$ **1** (mononuclear), $[Cu_3L^1(NO_3)_2]\cdot H_2O$ **2** (trinuclear), $[Cu_2L^1(NO_3)_2]$ **3** (sheet-like polymer) and $[Cu_2L^1(O_2CMe)_2]\cdot 2H_2O$ **4** (alternating chain). A comparative description of their magnetic properties is also included.

Experimental

Materials

Copper(II) nitrate trihydrate, acetate monohydrate, propane-1,3-diamine and diethyl oxalate were of reagent-grade quality obtained from commercial sources and used as received. The

† Oxamidato Complexes. Part 7.[1]
Non-SI unit employed: emu = *SI* × $10^6/4\pi$.

compound H_2L^1 was synthesized by reaction of propane-1,3-diamine and diethyl oxalate as described previously.[17] Elemental analyses (C, H, N) were performed by the Microanalytical Service of the Universidad Autónoma de Madrid (Spain). Copper contents was determined by atomic absorption spectrometry.

Preparations

[CuL^1] 1. Red crystals of complex **1** were obtained by evaporation of a filtered aqueous solution containing equimolar amounts of H_2L^1 and freshly prepared copper(II) hydroxide.[2,18] Rod-like single crystals of **1** were obtained from water–MeOH–CH_2Cl_2 (1 : 1 : 1) (0.5 mmol of **1**, 30 cm^3) by slow evaporation at room temperature (Found: C, 36.35; H, 6.05; Cu, 24.00; N, 21.10. Calc. for $C_8H_{16}CuN_4O_2$: C, 36.45; H, 6.10; Cu, 24.10; N, 21.25%).

[$Cu_3L^1_2(NO_3)_2$]·H_2O 2. This compound was isolated as a yellowish green polycrystalline powder by slow evaporation of a green solution containing stoichiometric amounts of **1** (2 mmol) and $Cu(NO_3)_2·3H_2O$ (1 mmol) dissolved in MeCN–water (4:1, 50 cm^3). The solid was washed with the minimum volume of cold water, ethanol and diethyl ether. Yield *ca.* 85%. All attempts to grow single crystals of **2** were unsuccessful (Found: C, 26.50; H, 4.20; Cu, 25.90; N, 19.05: Calc. for $C_{16}H_{34}Cu_3N_{10}O_{11}$: C, 26.20; H, 4.65; Cu, 26.00; N, 19.10%).

[$Cu_2L^1(NO_3)_2$] 3. Sky blue hexagonal plates of complex **3** suitable for X-ray analysis were grown from a dark blue MeOH–water (4:1, 50 cm^3) containing stoichiometric amounts of **1** (1 mmol) and $Cu(NO_3)_2·3H_2O$ (1 mmol) by slow evaporation at room temperature. They were filtered off, washed with cold water and air dried. The yield was practically quantitative (Found: C, 21.25; H, 3.50; Cu, 28.05; N, 18.55. Calc. for $C_8H_{16}Cu_2N_6O_8$: C, 21.30; H, 3.55; Cu, 28.15; N, 18.60%).

[$Cu_2L^1(O_2CMe)_2$]·$2H_2O$ 4. Dark blue prismatic crystals of complex **4** suitable for X-ray diffraction were obtained by slow evaporation of purple aqueous solutions (50 cm^3) containing stoichiometric amounts of **1** (1 mmol) and $Cu(O_2CMe)_2·H_2O$ (1 mmol). They were filtered off, washed with water and air dried. The yield was practically quantitative (Found: C, 30.20; H, 5.30; Cu, 26.10; N, 11.40. Calc. for $C_{12}H_{26}Cu_2N_4O_8$: C, 29.95; H, 5.40; Cu, 26.40; N, 11.65%).

Physical techniques

The infrared spectra were recorded on a Perkin-Elmer 1750 FTIR spectrophotometer as KBr pellets in the 4000–300 cm^{-1} region, electronic spectra in the solid state as Nujol mulls with a Perkin-Elmer Lambda 9 spectrophotometer. The magnetic susceptibility measurements were carried out on polycrystalline samples of complexes **1–4** in the temperature ranges 4.2–290 (**1**), 60–295 (**2**) and 80–290 K (**3**, **4**) with a fully automatized AZTEC DSM8 pendulum-type susceptometer[19] equipped with a TBT continuous-flow cryostat and a Brüker BE15 electromagnet operating at 1.8 T. The apparatus was calibrated with Hg[Co(NCS)$_4$]. Diamagnetic corrections were estimated from Pascal's constants[20] as -130×10^{-6}, -323×10^{-6}, -180×10^{-6} and -215×10^{-6} cm^3 mol^{-1}, respectively. Magnetic susceptibility data were also corrected for temperature-independent paramagnetism (-60×10^{-6} cm^3 per Cu^{II}) and magnetization of the sample holder.

Crystallography

Crystals of dimensions 0.70 × 0.45 × 0.40 (**1**), 0.65 × 0.55 × 0.40 (**3**) and 0.60 × 0.50 × 0.45 mm (**4**) were mounted on a Philips PW 1100 four-circle diffractometer and used for data collection. Intensity data were collected at 18 °C by using graphite-monochromated Mo-Kα radiation (λ = 0.710 73 Å) with the ω–2θ scan method. The scan width was $(p + 0.34 \tan\theta)°$ with p = 1.3 (**1**), 1.0 (**3**) and 0.9 (**4**). The unit-cell parameters were determined from least-squares refinements of the setting angles of 25 well centred reflections in the range θ 16–17°. Information concerning crystal parameters and structure refinements is summarized in Table 4. No significant fluctuations were observed in the intensities of two standard reflections monitored periodically. Intensity data were corrected for Lorentz-polarization and absorption effects.[21] The introduction of a secondary extinction coefficient was unnecessary. Of the 945 (**1**), 1321 (**3**) and 1627 (**4**) measured independent reflections, 588, 901 and 1092 were unique with $I \geqslant 3\sigma(I)$ and used for the structure refinements.

The structures were solved by direct (**1**) and Patterson (**3**, **4**) methods followed by successive Fourier syntheses and least-squares refinements on F (70, 114 and 119 parameters for **1**, **3** and **4**, respectively). The computations were performed with the program CRYSTALS[22] adapted on a MicroVax II computer. Non-hydrogen atoms were treated anisotropically. All hydrogen atoms were located on difference maps; their positions were not refined and they were given an overall isotropic thermal parameter. The ligand in **4** is disordered: atom C(3) occupies two positions with occupancy factors of 0.78 and 0.22. The hydrogen atoms corresponding to occupancy 0.78 were found on difference maps. Full-matrix least-squares refinements were carried out by minimizing the function $\Sigma w(||F_o| - |F_c||)^2$ and each reflection was assigned a unit weight. Atomic scattering factors for neutral Cu, O, N, C and H were taken from ref. 23. Anomalous dispersion was taken into account. Models reached convergence with values of the R and R' indices listed in Table 4. Criteria for satisfactory complete analysis were the ratios of the root mean square (rms) shift to standard deviation being less than 0.1 and no significant features in final difference maps. The residual maxima and minima in the final Fourier-difference maps were 0.50 and -0.38 e Å^{-3} for complex **1**, 0.39 and -0.29 e Å^{-3} for **3** and 0.37 and -0.31 e Å^{-3} for **4**. The molecular plots were drawn with the CAMERON[24] program. Final fractional coordinates for non-hydrogen atoms are listed in Tables 5 (**1**), 6 (**3**) and 7 (**4**) and main interatomic bond distances and angles in Tables 1 (**1**), 2 (**3**) and 3 (**4**).

Complete atomic coordinates, thermal parameters and bond lengths and angles have been deposited at the Cambridge Crystallographic Data Centre. See Instructions for Authors, *J. Chem. Soc., Dalton Trans.*, 1996, Issue 1.

Results and Discussion

Structures

[CuL^1] 1. The structure of complex **1** is composed of neutral mononuclear [CuL^1] units which are linked together by hydrogen bonds (see end of Table 1), forming sheets along the *ab* plane. A perspective view of the mononuclear entity with the atomic numbering scheme is depicted in Fig. 1(*a*) whereas its arrangement in the unit cell together with the hydrogen-bonding interactions are shown in Fig. 1(*b*).

The co-ordination of the copper(II) ion is nearly square planar, involving the four nitrogen atoms of the ligand [deviations from the CuN(1)N(1^I)N(2)N(2^I) mean plane are ± 0.178 Å for N(1) and N(1^I) and ± 0.165 Å for N(2) and N(2^I), the metal atom showing no deviation]. The copper atom lies in a binary axis, so the ligand L^1 presents a C_2 symmetry. The amine nitrogen-to-copper bond length [1.999(7) Å] is significantly longer than that involving the deprotonated amidate nitrogen [1.955(6) Å] consistent with the greater basicity of the latter. The ligand adopts the *cis* conformation and acts in a tetradentate manner forming one five- and two six-membered chelate rings. The distortion of the metal

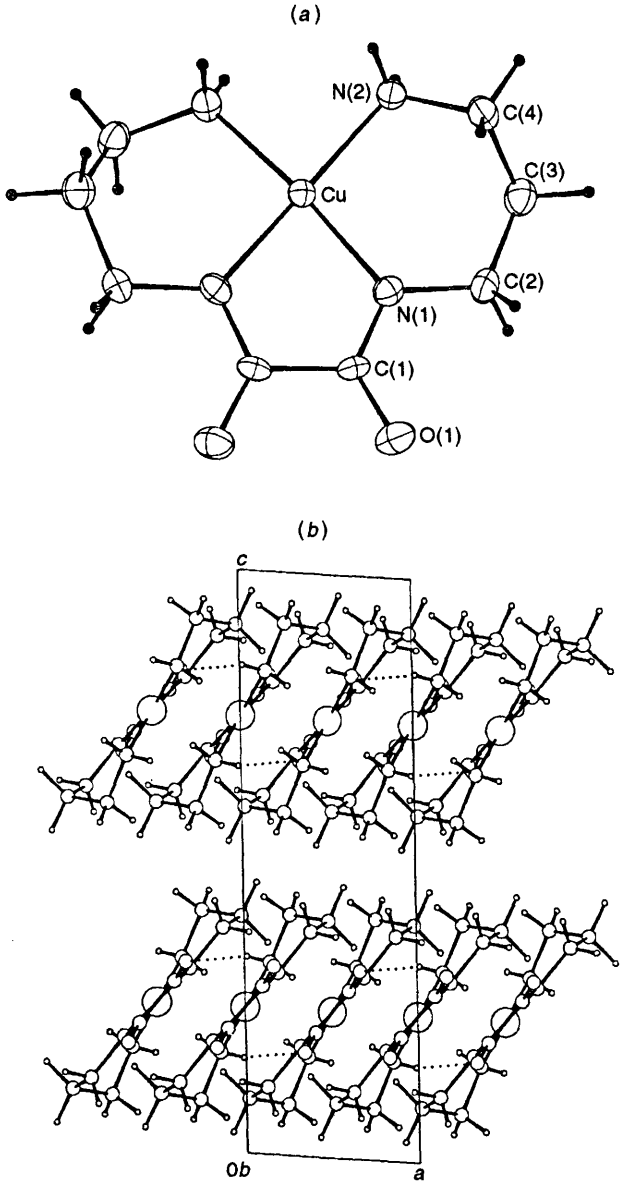

Fig. 1 (*a*) Perspective view of complex **1** with the atom numbering scheme. Thermal ellipsoids are drawn at the 30% probability level. (*b*) Projection of the unit cell along its *ab* plane showing the polymerization of the mononuclear units through hydrogen bonds (broken lines)

environment is evident from the deviation from the ideal 90° value found for the N(1)–Cu–N(1^{I}) and N(1)–Cu–N(2) angles [83.8(4) and 94.2(2)°, respectively] which belong to two adjacent five- and six-membered chelate rings. These chelate rings are far from being planar, the maximum deviations from the average planes being 0.043 Å [C(1^{I})] for CuN(1)C(1^{I})N(1^{I}) and −0.374 Å [C(3)] for CuN(1)C(2)C(3)C(4)N(2). The dihedral angle between these two mean planes is 11.7°. The C(1)–C(1^{I}) bond distance [1.50(1) Å] lies in the range observed [1.498(9)–1.511(9)] for di- and tri-nuclear copper(II) complexes containing the CuL^{1} unit as ligand.[2,3] However, significant differences are observed in the bond lengths within the N–C–O amidate fragment when comparing the structure of the uncoordinated [CuL^{1}] with those where it acts as a bidentate ligand towards copper(II): the co-ordination of [CuL^{1}] through its two carbonyl-carbon atoms leads to a shortening of the N–C bond (*ca.* 0.02 Å) and to a lengthening of the C–O distance (*ca.* 0.04 Å). The shortest metal–metal separation (4.911 Å) corresponds to the translation along the *a* axis.

$[Cu_2L^{1}(NO_3)_2]$ 3. The structure of complex **3** is made up of dinuclear centrosymmetric $[Cu_2L^{1}(NO_3)_2]$ units [Fig. 2(*a*)]

Table 1 Interatomic distances (Å) and angles (°) for compound **1** with estimated standard deviations (e.s.d.s) in parentheses *

Copper environment			
Cu–N(1)	1.955(6)	Cu–N(2)	1.999(7)
N(1)–Cu–N(1^{I})	83.8(4)	N(2)–Cu–N(1)	94.2(2)
N(2)–Cu–N(1^{I})	169.6(3)	N(2)–Cu–N(2^{I})	89.5(4)
C(1)–N(1)–Cu	113.0(5)	C(2)–N(1)–Cu	129.3(5)
C(4)–N(2)–Cu	118.2(5)		
Ligand L^{1}			
N(1)–C(1)	1.311(9)	N(1)–C(2)	1.45(1)
N(2)–C(4)	1.47(1)	O(1)–C(1)	1.254(8)
C(1)–C(1^{I})	1.50(1)	C(2)–C(3)	1.51(1)
C(3)–C(4)	1.50(1)		
O(1)–C(1)–N(1)	126.0(7)	C(1^{I})–C(1)–N(1)	114.8(4)
C(1^{I})–C(1)–O(1)	119.2(4)	C(3)–C(2)–N(1)	114.1(7)
C(4)–C(3)–C(2)	113.5(7)	C(3)–C(4)–N(2)	111.1(7)
C(2)–N(1)–C(1)	117.2(7)		

Hydrogen bonds

A	D	H	A···D	A···H–D
O(1^{II})	N(2)	H(2)	2.898(8)	164

* Symmetry codes: I $-x, y, \frac{1}{2}-z$; II $x-\frac{1}{2}, y+\frac{1}{2}, z$.

where L^{1} acts as a bis(terdentate) ligand and the nitrate groups are bound to the copper atoms in a bis (monodentate) fashion [Fig. 2(*b*)] yielding a layered network.

The environment of each copper atom is distorted square pyramidal, CuN_2O_3. The basal plane comprises the carbonyl oxygen O(1), amide N(1) and amine N(2) nitrogen atoms of the oxamidate ligand and a nitrate oxygen O(2) atom. These four atoms are displaced by 0.070 Å [N(1) and O(2)] below and 0.064 [N(2)] and 0.076 Å [O(1)] above the mean basal plane. The O(1)–Cu(1)–N(2) and O(2)–Cu(1)–N(1) angles are 177.2(2) and 167.5(2)°, respectively. The axial co-ordination site is occupied by another oxygen atom O(3^{II}) of a nitrate group which is equatorially bound to the neighbouring copper atom [Cu(1^{II})]. Each copper atom is displaced out of the equatorial plane toward the axial oxygen by 0.076 Å. The two Cu–O(nitrate) bonds are markedly different from each other, the equatorial being 2.001(4) Å and the axial 2.592(5) Å. The other three basal distances [1.925(5), 1.971(4) and 1.977(5) Å for Cu(1)–N(1), Cu–O(1) and Cu(1)–N(2), respectively] are close to those observed in parent oxamidato-bridged copper(II) complexes.[1,8,13–16,25] The significant shortening of the Cu(1)–N(1) bond length is in agreement with the stronger basicity of the deprotonated amide nitrogen atom.

The bis(terdentate) character of the ligand L^{1} produces one five- and one six-membered chelate ring on each copper atom, the angle subtended at the metal atom by the latter being larger [97.9(2)° for N(2)–Cu(1)–N(1)] than the former [84.9(2)° for O(1)–Cu(1)–N(1)]. The three atoms around N(1) lie in a plane with the bond angles 113.5(4), 118.8(5), 127.7(4)° for C(1^{I})–N(1)–Cu(1), C(2)–N(1)–C(1^{I}) and C(2)–N(1)–Cu(1), respectively. This fact together with the values of the bond lengths involved and the planarity of the N(1)C(1^{I})O(1^{I})-C(1)N(1^{I})O(1) oxamidate skeleton reveal that the amidate nitrogens are sp^2-hybridized and that the π-carbonyl electrons are delocalized to form a conjugated system. The length of C(1)–C(1^{I}) [1.52(1) Å] is very close to that observed in other two L^{1}-bridged (*trans* conformation) copper(II) dinuclear complexes $[Cu_2L^{1}(Him)_2(ClO_4)_2(H_2O)_2]$ [1.501(9) Å] (Him = imidazole) and $[Cu_2L^{1}{}_2(N_3)_2]\cdot 2H_2O$ [1.508(9) Å].[13] The N(1)O(1)-C(1)C(1^{I})O(1^{I})N(1^{I}) oxamidate plane and the mean equatorial plane of Cu(1) form a dihedral angle of 5.2°. The dihedral angle between this latter mean plane and the symmetry-related one of Cu(1^{II}) is 63.8°. The nitrate group is planar as expected. The

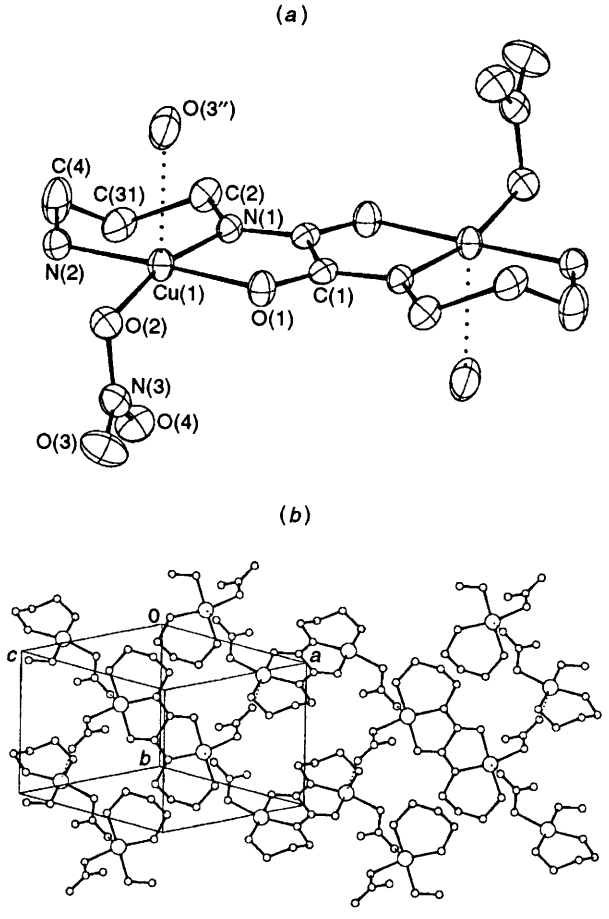

Fig. 2 (*a*) Perspective view of complex **3** with the atom numbering scheme. Thermal ellipsoids are drawn at the 30% probability level. (*b*) View of the unit-cell contents showing the occurrence of layers parallel to the 101 plane. The hydrogen atoms have been omitted for clarity. The dotted lines indicate weak axial co-ordination

lengthening of the N(3)–O(2) bond [1.284(6) Å] with respect to the other two intra-anion bond distances [1.226(6) and 1.228(6) Å for N(3)–O(3) and N(3)–O(4), respectively] is due to its strong co-ordination to copper through O(2).

The copper–copper separation through the ligand L^1 is 5.190(1) Å whereas there are two other equivalent Cu(1)···Cu(1^{II}) and Cu(1)···Cu(1^{III}) distances (symmetry code: III = $-\frac{1}{2} - x, -\frac{1}{2} + y, \frac{1}{2} - z$) of 5.116(1) Å between copper atoms bridged by the nitrate group.

$[Cu_2L^1(O_2CMe)_2]\cdot 2H_2O$ 4. The crystal structure of complex **4** consists of neutral zigzag chains of copper(II) ions bridged by L^1 and acetate groups. The former acts as bis(terdentate) ligand as in **3**, whereas the latter bridges the copper atoms in an asymmetrical end-on fashion. A perspective view of the asymmetric unit and of six symmetry-related units is depicted in Fig. 3(*a*). Inversion centres positioned at the middle of the C(1)–C(1^I) bond and Cu(1)···Cu(1^{II}) distance lead to chains of metal atoms running parallel to the *c* axis as shown in Fig. 3(*b*). These chains are linked by hydrogen bonds involving a water molecule of crystallization, the acetate oxygen O(3) and the amine nitrogen N(2) atoms (see end of Table 3).

The co-ordination environment around each copper atom can be described as a distorted square pyramid CuN_2O_3. The basal plane comprises the carbonyl oxygen O(1), amide N(1) and amine N(2) nitrogen atoms of L^1 and an oxygen atom O(2) of an acetate group. This same O(2) atom occupies the apical position for another symmetry related copper atom Cu(1^{II}). The two copper–acetate oxygen bonds are markedly different [1.957(4) and 2.456(4) Å for Cu(1)–O(2) and Cu(1)–O(2^{II}), respectively]. The same co-ordination behaviour of acetate

Table 2 Selected interatomic distances (Å) and angles (°) for compound **3** with e.s.d.s in parentheses *

Copper environment			
Cu(1)–N(1)	1.925(5)	Cu(1)–N(2)	1.977(5)
Cu(1)–O(1)	1.971(4)	Cu(1)–O(2)	2.001(4)
Cu(1)–O(3^{II})	2.592(5)		
N(2)–Cu(1)–N(1)	97.9(2)	O(1)–Cu(1)–N(1)	84.9(2)
O(1)–Cu(1)–N(2)	177.2(2)	O(2)–Cu(1)–N(1)	167.5(2)
O(2)–Cu(1)–N(2)	91.2(2)	O(2)–Cu(1)–O(1)	86.0(2)
O(3^{II})–Cu(1)–N(1)	96.0(2)	O(3^{II})–Cu(1)–N(2)	96.0(2)
O(3^{II})–Cu(1)–O(1)	84.2(2)	O(3^{II})–Cu(1)–O(2)	91.6(2)
C(1^I)–N(1)–Cu(1)	113.5(4)	C(2)–N(1)–Cu(1)	127.7(4)
N(3)–O(2)–Cu(1)	106.9(3)	C(4)–N(2)–Cu(1)	118.2(4)
C(1)–O(1)–Cu(1)	110.5(3)		
Ligand L^1			
N(1)–C(1^I)	1.292(6)	N(1)–C(2)	1.477(7)
N(2)–C(4)	1.470(8)	O(1)–C(1)	1.275(6)
C(1)–C(1^I)	1.52(1)	C(2)–C(31)	1.55(1)
C(2)–C(32)	1.53(3)	C(4)–C(31)	1.44(1)
C(4)–C(32)	1.34(3)		
C(2)–N(1)–C(1^I)	118.8(5)	O(1)–C(1)–N(1^I)	128.9(5)
C(1^I)–C(1)–O(1)	117.4(6)	C(1^I)–C(1)–N(1)	113.7(6)
C(32)–C(2)–N(1)	110.0(12)	C(31)–C(2)–N(1)	109.3(5)
C(32)–C(4)–N(2)	123.8(14)	C(31)–C(4)–N(2)	115.1(6)
C(4)–C(32)–C(2)	124.4(23)	C(4)–C(31)–C(2)	116.4(6)

* Symmetry codes: I $-x, -y, -z$; II $-\frac{1}{2} - x, \frac{1}{2} + y, \frac{1}{2} - z$.

was observed in the alternating copper(II) chain $[Cu_2L^2(O_2CMe)_2]$.[14] The oxamidate–copper bond lengths follows the pattern observed in **3** [1.999(4), 1.982(5) and 1.966(5) Å for Cu(1)–O(1), Cu(1)–N(2) and Cu(1)–N(1), respectively]. The mean displacement of the four equatorial atoms from the mean basal plane is 0.11 Å, the copper atom being displaced out of this plane toward the axial oxygen by 0.027 Å. The O(1)–Cu(1)–N(2) and O(2)–Cu(1)–N(1) angles are 171.9(2) and 170.2(2)°, respectively. The distortion of the metal environment is also evident from the values of the angles subtended at the copper by the adjacent five- [83.3(3)° for O(1)–Cu(1)–N(1)] and six-membered [95.8(2)° for N(2)–Cu(1)–N(1)] chelate rings. The least-squares plane through the four closest donor atoms of Cu(1) [O(1)N(1)N(2)O(2)] forms a dihedral angle of 14.7° with the oxamidato plane [O(1)C(1)N(1^I)C(1^I)O(1^I)N(1)]. The distance between the mean plane Cu(1)O(1)N(1)N(2)O(2) and the symmetry-related one involving the Cu(1^{II}) atom is 2.308 Å. The mean planes Cu(1)O(1)N(1)N(2)O(2) and Cu(1)O(2)-Cu(1^{II})O(2^{II}) form a dihedral angle of 100.6°.

The copper–copper separations through the L^1 and acetate bridges are 5.244(1) and 3.350(1) Å respectively, whereas the shorter interchain metal–metal distance is 7.212(1) Å.

Infrared and electronic spectra

The relevant features of the IR spectrum of complex **1** are the presence of a sharp and intense doublet at 3190 and 3125 cm^{-1} due to the $\nu(NH_2)$ stretching vibrations, a very strong absorption at 1586 cm^{-1} which is assigned to the ν_{sym}(NCO) stretching vibration (amide I band), and two medium-intensity bands centred at 1350 and 710 cm^{-1} corresponding to ν_{sym}(NCO) stretching and δ(CO) deformation modes, respectively. The strong shift of the amide I band toward lower frequencies when compared to that of neutral H_2L^1 (1639 cm^{-1}) is due to the higher bond order of the carbonyl group in the latter [1.254(8) Å for O(1)–C(1) in **1** *versus* 1.228(1) Å for the related carbonyl bond of the oxamide-*N*,*N*′-diacetate].[26] In the IR spectrum of complex **2**, apart from the bands due to water [a sharp feature of medium intensity at 3440 cm^{-1} most likely due to the ν(OH) stretching of lattice water molecules][27] and free

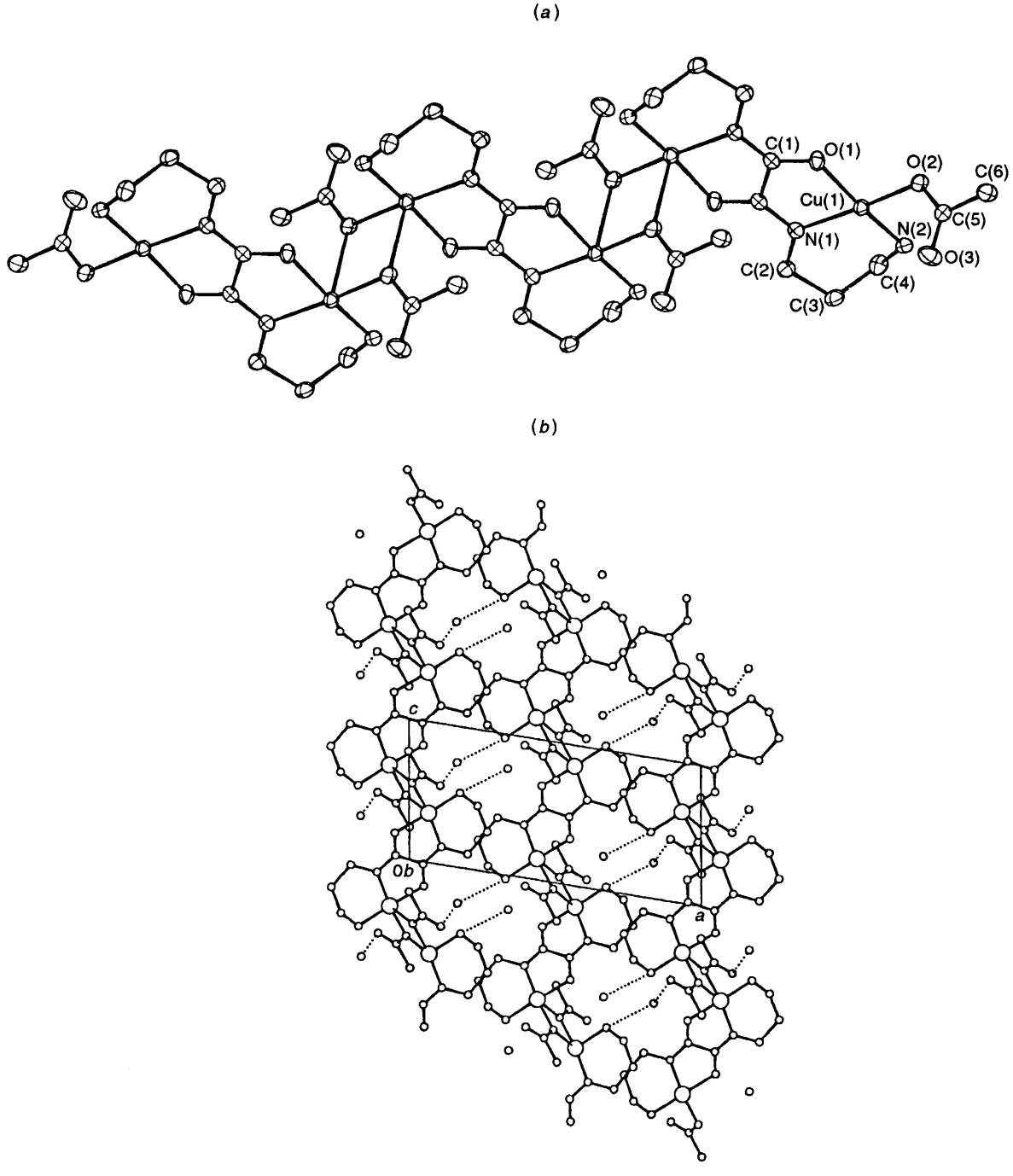

Fig. 3 (*a*) Perspective view of the asymmetric unit and of six symmetry-related units of complex **4** with the atom numbering scheme. Thermal ellipsoids are drawn at the 30% probability level. (*b*) A projection of the unit cell through the *b* axis showing the parallel alignment of the chains along the *c* axis. Dotted lines indicate hydrogen bonds between the chains and the water molecule of crystallization

nitrate (two weak absorptions at 2430 and 830 cm^{-1} and a strong one at 1385 cm^{-1}),[28] the most relevant absorptions are the occurrence of a medium-intensity doublet at 3210 and 3100 cm^{-1} [$\nu(NH_2)$ stretching vibrations] and a sharp and intense peak at 1620 cm^{-1} (amide I band). It is interesting that the $\delta(CO)$ deformation mode observed for **1** is lacking in the infrared spectrum of **2**. The shift of the amide I band to higher frequencies for **2** as compared to that for **1** has been used as definite proof for the existence of the oxamido bridge.[29] Moreover, the fact that the $\delta(CO)$ mode is not present in the spectrum of **2** has been attributed to co-ordination of the carbonyl oxygen of **1** to a second metal ion.[6] These spectral features together with the analytical and magnetic (see below) data for **2** support a trinuclear structure for it with two terminal CuL^1 units acting as bidentate ligands toward a central copper(II) ion. The IR spectra of **3** and **4** have in common the occurrence of a sharp and strong absorption at 1610 cm^{-1} (amide I band) and medium-intensity peak at 1310 cm^{-1} [$\nu_{sym}(NCO)$ stretching vibration] as well as a medium-intensity quadruplet at 3300, 3250, 3210 and 3180 cm^{-1} [$\nu(NH_2)$ stretching vibrations]. The presence in both complexes of bis(terdentate) oxamidate accounts for this similarity. Again the shift toward higher frequencies of the amide I band is consistent with oxamidate bridging. It is interesting that the position of the amide I band is sensitive to the different co-ordination modes of L^1 in its copper(II) complexes: for neutral H_2L it is located at 1639 cm^{-1}, at 1586 cm^{-1} for **1** (tetradentate L^1, *cis* conformation), at 1620 cm^{-1} for **2** [bridging, L^1, *cis* conformation] and at 1610 cm^{-1} for **3** and **4** [bis(terdentate) L^1, *trans* conformation]. Given that the amide I band is due to a composite NCO oxamide vibration, differences in the bond order of the NCO skeleton when going from H_2L^1 to its metal

complexes through deprotonation and metal co-ordination would account for the shifting of this band.[4] Finally, a comparison between the $\nu(NH_2)$ stretching vibrations (number and position of the peaks) of **1** and **2** *versus* **3** and **4** reveals that they can be used to differentiate between the *cis* (**1** and **2**) and *trans* (**3** and **4**) conformations of the L^1 ligand: two peaks in the range 3210–3100 cm^{-1} (**1** and **2**) and four peaks between 3300 and 3180 cm^{-1} (**3** and **4**).

The reflectance spectrum of complex **1** shows a maximum at 490 nm which is assigned to a d–d band in the strong ligand field corresponding to the square planar CuN_4 chromophore. The visible spectrum of **2** reveals the presence of two maxima centred at 425 and 600 nm. The former may be attributed to a metal-to-ligand charge-transfer band whereas the latter is most likely due to the sum of the d–d transitions from the CuN_4 chromophore of the peripheral CuL^1 ligand and the CuO_4 chromophore of the central copper(II) ion. The significant shift toward lower frequencies of the d–d band of the CuN_4 chromophore in **2** in comparison to **1** is caused by the weakening of the ligand field due to co-ordination of the carbonyl oxygens of complex **1** in **2**. The visible spectra of **3** and **4** show a broad d–d band at 615 and 650 nm, respectively. The presence of the same chromophore CuN_2O_3 in both complexes accounts for their spectral similarity. The adoption of the *trans* conformation of the oxamidate ligand in **3** and **4** (weaker ligand field than that of tetradentate L^1) produces the red shift of the d–d absorptions in the visible spectra.

Table 3 Selected interatomic distances (Å) and angles (°) for compound **4** with e.s.d.s in parentheses *

Copper environment			
Cu(1)–O(1)	1.999(4)	Cu(1)–O(2)	1.957(4)
Cu(1)–N(1)	1.966(5)	Cu(1)–N(2)	1.982(5)
Cu(1)–O(2^{II})	2.456(4)		
O(1)–Cu(1)–N(1)	83.3(2)	O(1)–Cu(1)–O(2)	88.5(2)
O(1)–Cu(1)–N(2)	171.9(2)	O(1)–Cu(1)–O(2^{II})	84.8(2)
O(2)–Cu(1)–N(2)	92.9(2)	O(2)–Cu(1)–N(1)	170.2(2)
O(2)–Cu(1)–O(2^{II})	81.9(2)	N(2)–Cu(1)–N(1)	95.8(2)
N(2)–Cu(1)–O(2^{II})	87.5(2)	N(1)–Cu(1)–O(2^{II})	102.9(2)
Cu(1)–O(2)–Cu(1^{II})	98.1(1)		
Ligand L^1			
O(1)–C(1)	1.281(5)	C(1)–C(1^{I})	1.543(9)
C(1^{I})–N(1)	1.283(6)	N(1)–C(2)	1.471(6)
C(2)–C(3)	1.520(8)	C(3)–C(4)	1.514(8)
C(4)–N(2)	1.473(8)		
Cu(1)–O(1)–C(1)	110.8(3)	O(1)–C(1)–N(1^{I})	129.4(5)
O(1)–C(1)–C(1^{I})	116.3(6)	N(1^{I})–C(1)–C(1^{I})	114.3(6)
Cu(1)–N(1)–C(1^{I})	113.0(4)	Cu(1)–N(1)–C(2)	129.1(4)
C(2)–N(1)–C(1^{I})	110.8(3)	N(1)–C(2)–C(3)	112.0(5)
C(2)–C(3)–C(4)	113.8(5)	C(3)–C(4)–N(2)	111.6(5)
C(4)–N(2)–Cu(1)	115.8(4)		

Hydrogen bonds

A	D	H	A···D	A···H–D
O(4^{III})	N(2)	H(2)	2.991(7)	140
O(3)	O(4^{II})	H(4^{II})	2.832(7)	152

* Symmetry codes: I $-x, -y, -z$; II $-x, 1-y, -1-z$; III $x-\frac{1}{2}, \frac{1}{2}-y, z-\frac{1}{2}$.

Magnetic properties

The magnetic behaviour of complex **1** corresponds to a Curie law consistent with its monomeric nature. The $\chi_m T$ product at room temperature is equal to 0.41 cm^3 K mol^{-1} and it remains constant until 4.2 K. The calculated g value is then 2.10, in agreement with that obtained from the EPR spectrum of a polycrystalline sample of **1** at 4.2 K (axial doublet with $g_{\|} < g_{\perp}$ and $g = 2.09$).[6]

The temperature dependence of the $\chi_m T$ product of complex **2** is shown in Fig. 4. The value of $\chi_m T$ at room temperature is 0.634 cm^3 K mol^{-1}, is significantly smaller than that calculated for three non-interacting copper(II) ions, revealing the occurrence of strong antiferromagnetic coupling through the oxamidate bridge. The $\chi_m T$ value quickly decreases on cooling and attains a constant value of 0.408 cm^3 K mol^{-1} at temperatures lower than 90 K. The presence of such a plateau is the signature of the occurrence of a low-lying doublet. Given that the analytical, spectroscopic and magnetic data are consistent with the trinuclear nature of **2**, we have used the spin Hamiltonian (1) to describe its magnetic behaviour, where J

$$\hat{H} = -J(\hat{S}_1\cdot\hat{S}_2 + \hat{S}_3\cdot\hat{S}_2) - j(\hat{S}_1\cdot\hat{S}_3) + \beta[(g_1\hat{S}_1 + \hat{S}_3) + g_2\hat{S}_2]\cdot H \quad (1)$$

and j correspond to the exchange coupling parameters between adjacent and terminal copper(II) ions, respectively. Given that a

Table 5 Final atomic coordinates for compound **1** with e.s.d.s in parentheses

Atom	X/a	Y/b	Z/c
Cu	0.0	0.3527(1)	0.25
N(1)	0.188(1)	0.2465(5)	0.3119(4)
N(2)	0.145(1)	0.4564(5)	0.3290(4)
O(1)	0.166(1)	0.0804(4)	0.3222(4)
C(1)	0.100(1)	0.1600(5)	0.2879(4)
C(2)	0.379(2)	0.2510(6)	0.3851(6)
C(3)	0.484(2)	0.3523(7)	0.4059(5)
C(4)	0.261(2)	0.4263(6)	0.4125(5)

Table 4 Summary of crystal data[a] for $[CuL^1]$ **1**, $[Cu_2L^1(NO_3)_2]$ **3** and $[Cu_2L^1(O_2CMe)_2]\cdot 2H_2O$ **4**

Compound	**1**	**3**	**4**
Formula	$C_8H_{16}CuN_4O_2$	$C_8H_{16}Cu_2N_6O_8$	$C_{12}H_{26}Cu_2N_4O_8$
M	263.78	451.33	481.44
Space group	$C2/c$	$P2_1/n$	$P2_1/n$
a/Å	4.911(3)	10.473(1)	15.117(5)
b/Å	13.705(3)	7.625(1)	8.606(1)
c/Å	16.038(5)	9.519(3)	7.212(1)
β/°	94.24(1)	98.30(3)	99.36(2)
U/Å^3	1076(1)	752.2(5)	926(1)
Z	4	2	2
D_c/g cm^{-3}	1.63	1.99	1.73
$F(000)$	448	456	496
μ(Mo-Kα)/cm^{-1}	20.20	28.9	23.5
θ range/°	2–25	1–25	1–25
R[b]	0.045	0.033	0.033
R'[c]	0.051	0.037	0.035

[a] Details in common: monoclinic, $T = 18$ °C, $I \geqslant 3\sigma(I)$. [b] $R = [\Sigma(||F_o| - |F_c||)/\Sigma|F_o|]$. [c] $R' = [\Sigma(||F_o| - |F_c||)^2/\Sigma w|F_o|^2]^{\frac{1}{2}}$.

Table 6 Final atomic coordinates for compound **3** with e.s.d.s in parentheses

Atom	*X/a*	*Y/b*	*Z/c*
Cu(1)	−0.206 07(7)	0.126 7(1)	0.084 29(7)
N(1)	−0.093 1(4)	0.184 9(6)	−0.051 3(5)
N(2)	−0.329 2(5)	0.322 7(7)	0.042 6(5)
N(3)	−0.379 9(5)	−0.111 9(8)	0.137 7(5)
O(1)	−0.089 3(4)	−0.074 3(5)	0.131 5(4)
O(2)	−0.319 6(4)	0.012 8(6)	0.209 7(4)
O(3)	−0.432 3(5)	−0.226 0(7)	0.200 0(5)
O(4)	−0.382 8(4)	−0.112 2(7)	0.008 3(4)
C(1)	−0.000 3(5)	−0.074 6(7)	0.053 1(5)
C(2)	−0.103 0(6)	0.335 4(8)	−0.150 0(6)
C(4)	−0.298 4(7)	0.461(1)	−0.054 8(8)
C(31)*	−0.244 5(8)	0.400(1)	−0.177 1(8)
C(32)*	−0.181(3)	0.482(4)	−0.094(3)

* Occupancy factors for C(31) and C(32) are 0.78 and 0.22, respectively.

Table 7 Final atomic coordinates for compound **4** with e.s.d.s in parentheses

Atom	*X/a*	*Y/b*	*Z/c*
Cu(1)	−0.065 92(5)	0.064 04(9)	−0.350 7(1)
N(1)	−0.109 1(3)	−0.011 0(6)	−0.123 9(6)
N(2)	−0.173 1(3)	−0.001 1(6)	−0.529 7(7)
O(1)	0.048 3(3)	0.098 7(5)	−0.172 7(5)
O(2)	−0.011 0(3)	0.164 3(5)	−0.547 3(5)
O(3)	−0.105 1(4)	0.359 5(6)	−0.558 4(7)
O(4)	0.163 7(3)	0.358 6(6)	−0.255 9(7)
C(1)	0.046 0(4)	0.031 6(6)	−0.015 7(8)
C(2)	−0.198 3(4)	−0.071 0(8)	−0.103 7(8)
C(3)	−0.265 5(4)	−0.052 6(9)	−0.283 5(9)
C(4)	−0.232 4(4)	−0.113 7(8)	−0.457 2(9)
C(5)	−0.043 2(4)	0.293 6(7)	−0.614 1(8)
C(6)	0.000 4(4)	0.364 0(7)	−0.768 6(9)

maximum value of $-j$ equal to 1.6 cm^{-1} was determined for the related complex $[(CuL^1)_2Zn(H_2O)_2][BPh_4]_2$[3] and keeping in mind that the $-J$ value is expected to be very large, we have neglected the term accounting for the interaction between the peripheral copper(II) ions. Thus $j = 0$ and assuming that the g factors of the terminal and central copper atoms are equal, the theoretical expression (2) is derived where g is the average g

$$\chi_m T = \frac{N\beta^2 g^2}{4kT}\left[\frac{1 + \exp(J/kT) + 10\exp(3J/2kT)}{1 + \exp(J/kT) + 2\exp(3J/2kT)}\right] \quad (2)$$

factor and N, β and k have their usual meanings. Least-squares fitting of the experimental data led to $J = -325$ cm^{-1}, $g = 2.09$ and $R = 6.0 \times 10^{-5}$ where R is the agreement factor defined as $\Sigma_i[(\chi_m T)_{obs}(i) - (\chi_m T)_{calc}(i)]^2/\Sigma_i[(\chi_m T)_{obs}(i)]^2$. The value of the antiferromagnetic coupling agrees well with that reported for the structurally characterized parent compound of formula $[Cu_3L^1(ClO_4)_2]$ ($J = -353.6$ cm^{-1}).[3]

The temperature dependence of the magnetic susceptibility per two copper(II) ions of complexes **3** and **4** is shown in Fig. 5. Both curves exhibit a behaviour characteristic of strong antiferromagnetic coupling. Looking at the structures of **3** and **4**, two different exchange pathways are possible, one through the ligand L^1 and the other through the nitrate (**3**) or through the acetate (**4**) groups. Oxamidate ligands are known to be very effective in mediating antiferromagnetic coupling between copper(II) ions when the sets of oxygen and nitrogen donors occupy equatorial sites in the metal surroundings.[1,13,14,16,25c,h] This is the case for complexes **3** and **4**. The large σ in-plane overlap of the $d_{x^2-y^2}$ magnetic orbitals of each metal atom [the x and y axes are roughly defined by the N(1)–Cu(1)–O(2) and N(2)–Cu(1)–O(1) bonds, respectively] through the planar oxamidate bridge is at the origin of this strong antiferromagnetic

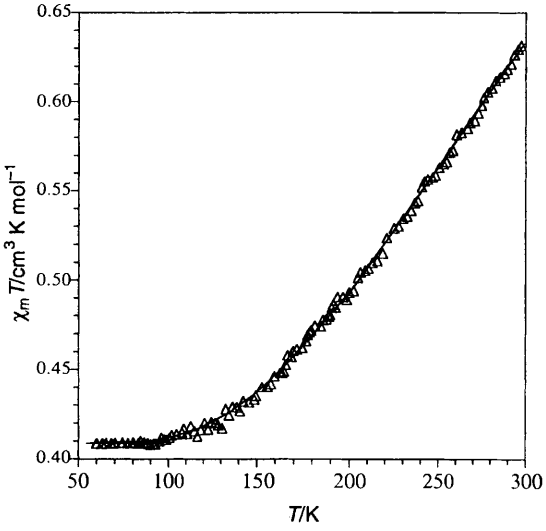

Fig. 4 Temperature dependence of the $\chi_m T$ product for complex **2**: (Δ) experimental data; (—) best theoretical fit

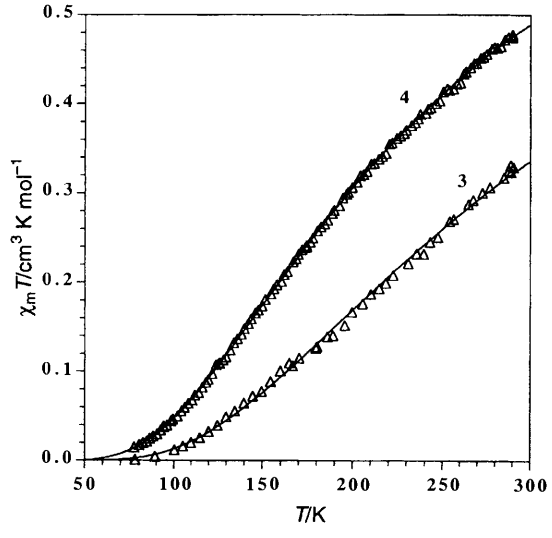

Fig. 5 Temperature dependence of the $\chi_m T$ product for complexes **3** and **4**: (Δ) experimental data; (—) best theoretical fit

interaction. A very small spin density is expected in the apical positions of each metal atom in **3** and **4** because of the weak axial co-ordination of nitrate and acetate bridges. In fact, both bridging ligands are such that the magnetic orbitals on the two neighbouring copper(II) ions are parallel to each other in two different planes. Under these conditions the magnetic coupling between the two ions either through the nitrate or acetate bridges is predicted to be very small. Based on these considerations and from a magnetic point of view, **3** and **4** can be treated as isolated oxamidato-bridged copper(II) dimers. Their magnetic properties were thus analysed through a simple Bleaney–Bowers expression with application of the Hamiltonian $H = -JS_1 \cdot S_2$ where J stands for the singlet–triplet energy gap and $S_1 = S_2 = \frac{1}{2}$ (local spins). The relative parameters obtained by least-squares minimization are $J = -393$ cm^{-1}, $g = 2.04$ and $R = 4.1 \times 10^{-4}$ for **3** and $J = -305$ cm^{-1}, $g = 2.10$ and $R = 1.3 \times 10^{-4}$ for **4**. The calculated curves fit satisfactorily the experimental points as shown in Fig. 5. Taking into account the structures of **3** (sheet-like polymer) and **4** (alternating chain), we attempted to fit their magnetic data by a modification of the Bleaney–Bowers expression considering the intermolecular interactions J' between z neighbours by the means of a zJ' term, in a molecular field approach (**3**) and in the hypothesis of an alternating chain[30] (**4**). The intradimer J values obtained were not significantly different from the previous ones and there was no significant improvement of the

fits. Both the zJ' (**3**) and α (alternation parameter) (**4**) values were very close to zero, as expected. Therefore, the evolution of the magnetic properties of complexes **3** and **4** can be interpreted essentially in terms of the oxamidate-bridged copper(II) unit.

The strong antiferromagnetic coupling observed in complexes **3** and **4** is in agreement with that reported for other L^1 bridged copper(II) dimers where the oxamidate exhibits the *trans* conformation: values of J equal to -360.8 and -341.7 cm^{-1} were reported for the complexes $[Cu_2L^1(Him)_2(ClO_4)_2(H_2O)_2]$ and $[Cu_2L^1(N_3)_2]\cdot 2H_2O$.[13] The fact that the antiferromagnetic coupling in **4**, although strong, is somewhat lower than that of complex **3** can be easily explained on the basis of structural distortions. In this regard, one of the relevant factors is the value of the dihedral angle (γ) between the mean equatorial plane of the metal ion and the oxamidate plane:[31] the greater the value of γ the smaller is the antiferromagnetic coupling. The value of γ is 14.7° in **4** and 5.2° in **3** revealing that a greater planarity of the Cu(oxamidate)Cu network is achieved in **3**, consistent with its greater antiferromagnetic coupling.

In summary, the present work shows how the versatility of ligand L^1 can be used to prepare mononuclear (**1**) and trinuclear (**2**) (L^1 in *cis* conformation) as well as layered (**3**) and alternating chain (**4**) (L^1 in *trans* conformation) compounds. Suitable bridging units such as nitrate and acetate appear useful tools to polymerize the dinuclear $[Cu_2L^1]^{2+}$ entities yielding chain or sheetlike polymers. Finally, strong antiferromagnetic interactions can be obtained through the L^1 bridge adopting either the *cis* (**2**) or *trans* (**3** and **4**) conformations.

Acknowledgements

Financial support from the Direccíon General de Investigación Científica y Técnica (DGICYT) (Spain) through Project PB91-0807-C02-01 and the Human Capital and Mobility Program (Network on Magnetic Molecular Materials) through grant ERBCHXCT920080 is gratefully acknowledged. Two of us are indebted to the Conselleria de Cultura, Educació i Ciència de la Generalitat Valenciana (B. C.) and to the Ministerio de Educación y Ciencia (R. R.) (Spain) for pre- and post-doctoral grants, respectively.

References

1 Part 6, J. A. Real, M. Mollar, R. Ruiz, J. Faus, F. Lloret, M. Julve and M. Philoche-Levisalles, *J. Chem. Soc., Dalton Trans.*, 1993, 1483.
2 Y. Journaux, J. Sletten and O. Kahn, *Inorg. Chem.*, 1985, **24**, 4063.
3 Y. Journaux, J. Sletten and O. Kahn, *Inorg. Chem.*, 1986, **25**, 439.
4 H. Ojima and K. Nonoyama, *Coord. Chem. Rev.*, 1988, **92**, 85 and refs. therein.
5 Z. Y. Zhang, D. Z. Liao, Z. H. Jiang, S. Q. Hao, X. K. Yao, H. G. Wang and G. L. Wang, *Inorg. Chim. Acta*, 1990, **173**, 201.
6 F. Lloret, Y. Journaux and M. Julve, *Inorg. Chem.*, 1990, **29**, 3967.
7 (*a*) Z. M. Liu, D. Z. Liao, Z. H. Jiang and G. L. Wang, *Synth. React. Inorg. Met.-Org. Chem.*, 1991, **21**, 289; (*b*) Z. Y. Zhang, S. Q. Hao and G. L. Wang, *Abstracts XXVII International Conference on Coordination Chemistry*, Broadbeach, Queensland, 2–7 July, 1989.
8 F. Lloret, M. Julve, J. Faus, R. Ruiz, I. Castro, M. Mollar and M. Philoche-Levisalles, *Inorg. Chem.*, 1992, **31**, 784.
9 A. Escuer, R. Vicente, J. Ribas, R. Costa and X. Solans, *Inorg. Chem.*, 1992, **31**, 2627.
10 D. Z. Liao, L. C. Li, Z. H. Jiang, S. P. Yan, P. Cheng and G. L. Wang, *Transition Met. Chem. (Weinheim)*, 1992, **17**, 356.
11 C. Mathonière, O. Kahn, J. C. Davan, H. Hilbig and F. H. Köler, *Inorg. Chem.*, 1993, **32**, 4057.
12 J. L. Sanz, R. Ruiz, A. Gleizes, F. Lloret, J. Faus, M. Julve and A. Gleizes, *Inorg. Chem.*, submitted for publication.
13 Z. N. Chen, W. X. Tang and K. B. Yu, *Polyhedron*, 1994, **13**, 783.
14 A. Bencini, C. Benelli, A. C. Fabretti, G. Franchini and D. Gatteschi, *Inorg. Chem.*, 1986, **25**, 1063.
15 F. Lloret, M. Julve, J. A. Real, J. Faus, R. Ruiz, M. Mollar, I. Castro and C. Bois, *Inorg. Chem.*, 1992, **31**, 2956.
16 J. A. Real, R. Ruiz, J. Faus, F. Lloret, M. Julve, Y. Journaux, M. Philoche-Levisalles and C. Bois, *J. Chem. Soc., Dalton Trans.*, 1994, 3769.
17 H. J. Chang and O. Vogl, *J. Polym. Sci.*, 1977, **15**, 311.
18 H. Ojima and K. Nonoyama, *Z. Anorg. Allg. Chem.*, 1972, **389**, 75.
19 J. C. Bernier and P. Poix, *Actual. Chim.*, 1978, **2**, 7.
20 A. Earnshaw, *Introduction to Magnetochemistry*, Academic Press, London, New York, 1968.
21 N. Walker and D. Stuart, *Acta Crystallogr., Sect. A*, 1983, **39**, 158.
22 D. J. Watkin, J. R. Carruthers and P. W. Betteridge, CRYSTALS, An advanced crystallographic computer program system, Chemical Crystallographic Laboratory, University of Oxford, 1988.
23 *International Tables for X-Ray Crystallography*, Kynoch Press, Birmingham, 1974, vol. 4.
24 L. J. Pearce and D. J. Watkin, CAMERON, Crystallography Laboratory, Oxford.
25 (*a*) A. Yoshino and W. Nowacki, *Z. Krystallogr.*, 1974, **139**, 337; (*b*) J. Sletten, *Acta Chem. Scand., Ser. A*, 1982, **36**, 343; (*c*) A. Bencini, M. Di Vaira, A. C. Fabretti, D. Gatteschi and C. Zanchini, *Inorg. Chem.*, 1984, **23**, 1620; (*d*) M. Verdaguer, O. Kahn, M. Julve and A. Gleizes, *Nouv. J. Chim.*, 1985, **9**, 325; (*e*) F. Lloret, M. Julve, J. Faus, Y. Journaux, M. Philoche-Levisalles and Y. Jeannin, *Inorg. Chem.*, 1989, **28**, 3702; (*f*) H. Okawa, N. Matsumoto, M. Koikawa, K. Takeda and S. Kida, *J. Chem. Soc., Dalton Trans.*, 1990, 1383; (*g*) A. Cornia, A. C. Fabretti, F. Ferraro, D. Gatteschi and A. Giusti, *J. Chem. Soc., Dalton Trans.*, 1993, 3363; (*h*) J. P. Costes, F. Dahan and J. P. Laurent, *Inorg. Chim. Acta*, 1995, **230**, 199.
26 F. Lloret, J. Sletten, R. Ruiz, M. Julve, J. Faus and M. Verdaguer, *Inorg. Chem.*, 1992, **31**, 779.
27 K. Nakamoto, *Infrared and Raman Spectra of Inorganic and Coordination Compounds*, 4th edn., Wiley, New York, 1986, p. 228 and refs. therein.
28 M. R. Rosenthal, *J. Chem. Educ.*, 1973, **50**, 331.
29 H. Ojima and K. Nonoyama, *Z. Anorg. Allg. Chem.*, 1972, **389**, 75.
30 W. E. Hatfield, *J. Appl. Phys.*, 1981, **52**, 1985.
31 S. Alvarez, M. Julve and M. Verdaguer, *Inorg. Chem.*, 1990, **29**, 4500.

Received 3rd *October* 1995; *Paper* 5/06516J